Complex Modes in Boxed Microstrip

C. J. RAILTON AND T. ROZZI, SENIOR MEMBER, IEEE

Abstract—**Previously published results for the higher order modes of microstrip have been restricted to a few modes, whereas for the analysis of discontinuities as many as a hundred modes must be taken into account. A method of obtaining the propagation coefficients and field patterns of a large number of modes with a minimum of computational effort is described. This includes the "complex modes" recently reported in microstrip. In addition the characteristic impedance of microstrip is efficiently calculated.**

I. Introduction

THE ACCURATE analysis of microstrip discontinuities, including strongly coupled discontinuities, is an important requirement in the design of filters, stepped impedance transformers, and other microwave components. It becomes especially important in the design of microwave integrated circuits, where adjustments after fabrication are difficult or impossible to carry out.

The published methods for use in the computer-aided design of microstrip components, e.g. [1], [2], rely heavily on quasi-static approximations, which are only correct in the limit of low frequency. Attempts at obtaining more accurate results at higher frequencies have been made using a parallel-plate transmission line model in an attempt to take account of the higher order modes excited at the discontinuity. A comprehensive description of this method is given in [3]. The method is of limited accuracy, however, due to the different nature of the higher order modes in the model compared to those of the original structure.

Recently, a rigorous formulation for the microstrip step has been published [4] using a different formulation, which provides S parameters for many configurations but does not consider strong interactions. Modal matching has been used in [5] to study single and multiple steps such as filters.

In [6] the single-step discontinuity is analyzed using the Galerkin variational method. The E field at the discontinuity is expanded in the set of microstrip modes on each side of the step and in a suitable set of basis functions appropriate to the step itself. This method leads directly to variational principles for the multiport S parameters of the step. The form of the results is suitable for use in calculating the effect of coupled steps.

Manuscript received July 22, 1987; revised December 7, 1987.

C. J. Railton was with the School of Electrical Engineering, University of Bath, U.K. He is now with the Communications Research Group, Department of Electrical and Electronic Engineering, Bristol University, BS8 1TR, U.K.

T. Rozzi is with the School of Electrical Engineering, University of Bath, Bath BA2 7AY, United Kingdom.

IEEE Log Number 8819965.

In order to analyze a microstrip discontinuity in this way, it is necessary to calculate the field patterns of a large number of higher order modes, typically of the order of 100. The problem is essentially the location of the zeros of a characteristic equation. Because this equation also contains many poles, sometimes very close to the searched-for zeros, care must be taken not to miss solutions, on the one hand, or to necessitate the performance of prohibitive amounts of computation, on the other.

The method described herein uses a discrete space domain formulation to calculate a large number of higher order modes in a way which leads to their fast location and which ensures that no modes are missed. This includes those pairs of modes with complex conjugate propagation constants of the type which have been recently reported for finline [7] as well as the normal evanescent modes. It is entirely practicable to implement the computer program to perform these calculations on a "home computer."

By making use of the calculated field patterns, the characteristic impedance of the microstrip can be calculated. Much discussion has taken place in the literature concerning the application of the concept of characteristic impedance to microstrip and how it should be defined [11]–[15]. The results presented here are obtained using the generally accepted power–current definition and are in agreement with other published results.

II. Calculation of Higher Order Modes

The formulation uses Galerkin's method with the microstrip currents as the unknown functions. By using test functions with the appropriate edge conditions, it is shown that accurate solutions for a very large number of modes are obtained using a basis expansion of only two functions in the longitudinal current and the derivative of the transverse current in the strip. In addition, the field patterns can be accurately established. In all cases where the evaluation of an infinite series is involved, accurate values are obtained by use of asymptotic functions with easily calculated sums. A brief outline of the formulation now follows.

In the box cross section we can express the x- and z-directed components of the electric field in terms of the current in the strip as

$$\boldsymbol{E}(\boldsymbol{r}) = \langle \underline{\underline{G}}(\boldsymbol{r}, \boldsymbol{r}'), \boldsymbol{J}(\boldsymbol{r}') \rangle \tag{1}$$

where $\underline{\underline{G}}(\boldsymbol{r}, \boldsymbol{r}')$ is the dyadic Green's function for the structure and is given in Appendix II and $\boldsymbol{r} = (x, y)$.

0018-9480/88/0500-0865$01.00

The inner product $\langle a, b \rangle$ is defined as $\int a \cdot b \, dS$ and the integral is taken over the box cross section. When a and b are vectors the result is scalar, when $\underline{a}$ is a dyadic, the result is a vector.

We now expand the strip current in terms of a suitable basis function and substitute

$$E(r) = \sum_s a_s \langle \underline{G}(r, r'), J_s(r') \rangle. \tag{2}$$

Multiplying each side of the equation by any of the basis functions J_t and taking the inner product, we get a set of simultaneous equations from which the unknown coefficients a_s can be found:

$$\langle J_t, E(r) \rangle = \sum_s a_s \langle J_t, \underline{G}(r, r'), J_s(r') \rangle = 0. \tag{3}$$

The solutions of this set of homogeneous equations is found by setting the determinant of the matrix K equal to zero, where

$$K_{st} = \langle J_t(r), \underline{G}(r, r'), J_s(r') \rangle. \tag{4}$$

From the continuity conditions of the electric and magnetic fields at the air–dielectric interface, the Fourier transform of the dyadic Green's function can be derived [7]. A more general method by means of which the required function can be found for multilayer geometries is given in [7]. If the Fourier transforms of the basis functions are known, then the elements of K can be quickly found by summing the products of the Fourier coefficients:

$$K_{st} = \sum_n \tilde{J}_t(n) \cdot \underline{\tilde{G}}(n, \beta) \cdot \tilde{J}_s(n) \tag{5}$$

where the tilde denotes the Fourier transforms of $\underline{G}$ and J, which are given in Appendix I.

The computations can be speeded up by making use of asymptotic forms of $\underline{G}$ and J which have sums which either can be expressed in closed form or need be calculated only once for a particular geometry and then used each time K has to be calculated. As n approaches infinity, the value of $\underline{G}$ is given in Appendix II. The value of J in this limit will depend on the basis functions chosen to represent the current in the strip.

We express (5) as follows:

$$K_{st} = \sum_n \tilde{J}_t(n) \left(\underline{\tilde{G}}(n, \beta) - \underline{\tilde{G}}'(n, \beta) \right) \tilde{J}_s(n) + \sum_n \tilde{J}_t(n) \underline{\tilde{G}}'(n, \beta) \tilde{J}_s(n)$$

where $\underline{\tilde{G}}'$ is the asymptotic form of $\underline{\tilde{G}}$, given in Appendix II.

One can typically truncate the first summation after about ten terms. If (5) were used as it stands, then about 500 terms would have to be taken to ensure accuracy. Since during a search for zeros of $\det(K)$ the matrix K must be calculated many times, this saving is important. Examination of the dependence on n of the terms of the second summation shows that it can be written in the form

$$\sum_n \frac{J_t(n) \cdot \underline{H}(\beta) \cdot J_s(n)}{n}$$

where $\underline{H}(\beta)$ is given in Appendix II.

The above summation depends only on the ratio of the widths of the strip and the box and thus need be calculated only once for each microstrip geometry to be considered.

In order to get accurate results requiring the matrix K to be large, it is important to select a set of basis functions in which it is possible to accurately approximate the actual current using very few terms. It has been shown [9] that if the basis functions contain the correct edge singularity, then reasonable results for the propagation coefficients are obtained using even just one term. The basis functions which have been used here are

$$\tilde{J}_{zmr} = \tilde{J}'_{xmr} = \frac{T_m(2x_r/w_r)}{\sqrt{\left(1 - (2x_r/w_r)^2\right)}} \tag{6}$$

where

x_r displacement from the centre of the rth strip,
w_r width of the rth strip,
$T_m(x)$ Chebyshev polynomials.

These functions are appropriate for single or multiple strips placed anywhere on the air–dielectric interface and have the correct edge singularity. Their Fourier transforms are easily expressed in terms of Bessel functions. In addition, due to orthogonality, only the first term in the expansion of J_z contributes to the total longitudinal current.

Fig. 1 shows the convergence of the effective permittivity of the dominant mode as the number of basis functions is increased. Basis functions containing the edge singularity (6) and with no singularity (Legendre polynomials) are examined. The figure also shows the effect of expanding the aperture fields instead of the strip currents. It can be

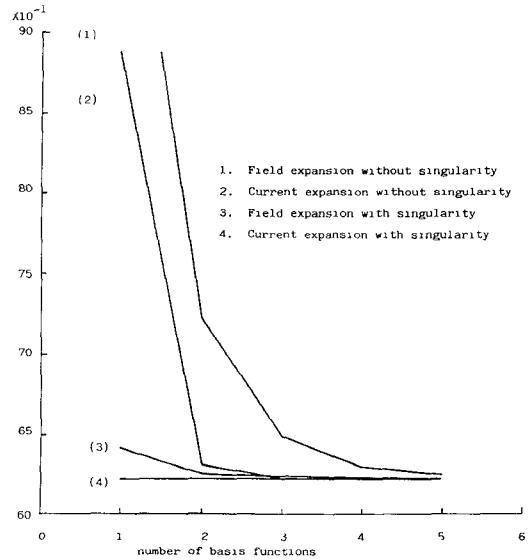

Fig. 1. Convergence with various basis functions.

seen that, with the correct singularity, convergence is very fast. Without the singularity convergence is relatively slow.

The accurate location of the modes is accomplished by making use of the fact that the poles of the characteristic equation correspond to the roots of the dispersion equation of a dielectric-slab-loaded waveguide. These are the solutions of the equation

$$XY = 0 \tag{7}$$

where $X = 0$ is the characteristic LSE equation for the slab-loaded guide and $Y = 0$ is the equation for the LSM case. The terms (X) and (Y) are defined in Appendix I.

Moreover, between any two poles there can be no more than two roots. That this is so can be shown by considering the form of the characteristic determinant. For the formulation in terms of the aperture fields this can be expressed as follows:

$$\det(\beta^2) = \sum_n \tilde{E}_x^2(n)\tilde{E}_z^2(n)(\alpha_n^2 + \beta^2)Y_e Y_h$$

where $\tilde{E}_x$ and $\tilde{E}_z$ are the Fourier transforms of the x and z components of the E field in the aperture and

$$Y_e = \frac{\tan k_n' h}{k_n'} + \frac{\epsilon_r \tan k_n d}{k_n}$$

$$Y_h = k_n' \tan k_n' h + k_n \tan k_n d.$$

The quantities k_n and k_n' are defined in Appendix II. By expanding the tangents we get

$$\det(\beta^2) = \sum_n R_n^2(\alpha_n^2 + \beta^2) \left\{ K_1 k_n^2 \sum_k \frac{1}{(2k-1)^2 - \left[\frac{2k_n d}{\pi}\right]^2} + K_2 k_n'^2 \sum_k \frac{1}{(2k-1)^2 - \left[\frac{2k_n' h}{\pi}\right]^2} \right\} * \left\{ K_3 \sum_k \frac{1}{(2k-1)^2 - \left[\frac{2k_n d}{\pi}\right]^2} + K_4 \sum_k \frac{1}{(2k-1)^2 - \left[\frac{2k_n' h}{\pi}\right]^2} \right\}$$

where $R_n = \tilde{E}_x(n)\tilde{E}_z(n)$. K_1, K_2, K_3, and K_4 are constants. Using the definitions of k_n and k_n' we can express the denominators of this expression thus:

$$f_{nk} - \beta^2$$

where f_{nk} is independent of β and the poles of $\det(\beta^2)$ are located at $\beta^2 = f_{nk}$.

We now consider the behavior of $\det(\beta^2)$ over the interval between two consecutive poles at $\beta^2 = f_{n1k1}$ and $\beta^2 = f_{n2k2}$. This will be dominated by the terms of the summation which give rise to the poles:

$$\det(\beta^2) = R_{n1}^2(\alpha_{n1}^2 + \beta^2)\frac{K_{n1}}{f_{n1k1} - \beta^2} + R_{n2}^2(\alpha_{n2}^2 + \beta^2)\frac{K_{n2}}{f_{n2k2} - \beta^2} + F(\beta^2)$$

where K_{n1} and K_{n2} are either constant or linear functions of β^2. $F(\beta^2)$ is made up of the other terms of the summation. Since $F(\beta^2)$ is made up of functions which are monotonically increasing or decreasing in the interval under consideration, it cannot introduce zeros into the derivative of $\det(\beta^2)$. For the purposes of investigating the existence of zeros it can be neglected. We are thus left with a quadratic in β^2 which will have two roots, each or neither of which may lie in the interval between the poles.

An analogous, although algebraically more involved, argument may be used for the formulation in terms of strip currents.

In addition, there is a one-to-one correspondance between the slab-loaded guide modes and the quasi-TE and quasi-TM modes of the microstrip. The number of roots of $\det(\beta^2)$ will therefore exceed the number of poles by 1. The extra root corresponds to the quasi-TEM mode.

If during a search of the real axis of the complex plane it is found that there are more poles than roots, then the existence of complex roots is indicated. Their approximate location can be ascertained by keeping a count of the number of poles minus the number or roots found as the search along the real axis proceeds. The exact positions of the roots can then be located by performing a search of the upper half of the complex plane. Once a root is found, it is known that its complex conjugate is also a root.

In a similar manner the initial location of the modes of the slab-loaded guide is facilitated by first locating the poles of expression (7). These occur when the argument of either of the tangent terms is an odd multiple of $\pi/2$ or the argument of either of the cotangent terms is an even multiple of $\pi/2$. In other words, we have a pole whenever

$$\epsilon_r k_0^2 - \beta^2 - \alpha_n^2 = (m\pi/2d)^2 \tag{8}$$

$$k_0^2 - \beta^2 - \alpha_n^2 = (m\pi/2h)^2 \tag{9}$$

for any integer value of n and m.

Thus the values of the propagation coefficient, beta, at which there is a pole in expression (7) can be found exactly by evaluating a simple analytic expression.

By these means the complete mode spectrum can be found with a comparatively small amount of computation. Indeed it is entirely practicable to implement the method on a Sinclair Spectrum computer with an available PASCAL compiler.

The formulation can easily be applied to finline or to multilayer structures. All that is necessary is to obtain the appropriate form of the Green's function using an extension of the method given in Appendix II or the method of

[9] and then find expressions for the poles of the characteristic equation in the above manner.

Once the propagation coefficient for a particular mode has been found, any of the corresponding field eigenvectors can be evaluated by means of the expressions given in Appendix II.

III. Characteristic Impedance of Microstrip

In the literature, e.g. [11]–[14], a great deal of discussion has taken place in regard to the definition of characteristic impedance for microstrip. Given the values of total transported power, total longitudinal current, and the voltage between the box and the strip, three separate definitions of characteristic impedance are possible. In addition we have the "reflection definition" [15], where the reflection at a discontinuity of microstrip with a waveguide of known characteristic impedance is calculated and this is used to define the characteristic impedance of microstrip.

Unfortunately, except in the limit of zero frequency, all these methods give different answers. Moreover as a function of frequency, some of these answers increase and some decrease.

This ambiguity is the direct result of the hybrid nature of the microstrip mode and the attempt to apply concepts appropriate to TEM lines of a quasi-TEM microstrip. Thus for a microstrip the concept of characteristic impedance is an approximate one.

It is generally accepted that the most physically meaningful approximation is the definition based on total transported power and total longitudinal current. This definition has been used in the following formulation.

Denoting the characteristic impedance by Z_0, we have

$$Z_0 = \frac{\langle E \times H^*, \hat{z} \rangle}{\left\{ \int J_z \, dx \right\}^2} \tag{10}$$

where * denotes complex conjugate.

Because of the form of the basis functions chosen for the longitudinal current in (6), the integral in the denominator of (10) becomes simply

$$a_0 \int_{-w_r/2}^{w_r/2} \frac{dx_r}{\sqrt{\left(1-(2x_r/w_r)^2\right)}} \tag{11}$$

where a_0 is the coefficient of the first term in the current eigenvector derived in the solution of (3). Due to the orthogonality properties of Chebyshev polynomials, this is the only term in the expansion of J_z to contribute to the integral.

The inner product in the numerator can be reduced, by applying Parseval's theorem, to a summation of the products of field terms, the derivation of which is given in Appendix II.

IV. Results for Uniform Microstrip

The following results were calculated using two basis functions for each current component.

The dispersion characteristics of the first 20 modes of the microstrip whose geometry is shown in Fig. 2 are shown in Fig. 3. These were calculated using a modest amount of computer power.

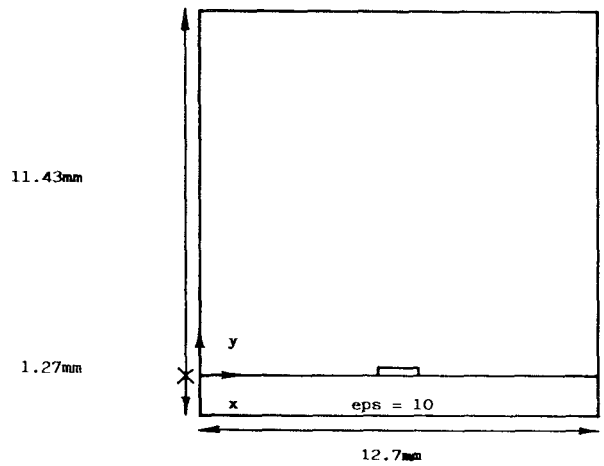

Fig. 2. Microstrip cross section.

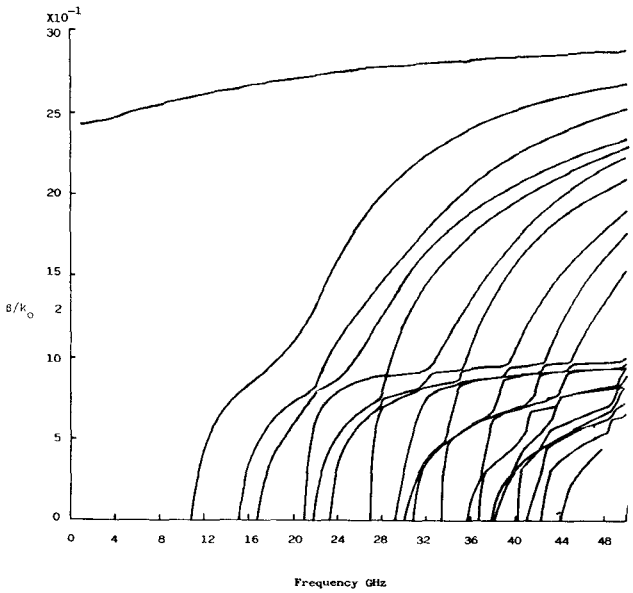

Fig. 3. Higher order modes of microstrip. $a = 12.7$ mm: $d = 1.27$ mm; $h = 10.43$ mm; $w = 1.27$ mm; eps = 8.875.

The E field intensity over the box cross section for the dominant mode and for mode 20 are shown in an isometric projection in Fig. 4. It can be seen that the expected singularity exists at the strip edge. It can also be seen that the field is concentrated at the air–dielectric interface.

Using the geometry given in Fig. 2 at a frequency of 5 GHz, modes 18 and 19 have been found to have complex conjugate propagation constants with strip widths in the region of 0.5 mm–2 mm. Fig. 5 shows the locus of these modes as the strip width varies. Also shown are the adjacent modes, the 17th and 20th, and the modes of a slab-loaded guide formed by removing the strip; the latter are the vertical lines. It can be seen that the phase of the propagation constant becomes large where the locus crosses the position of a slab guide mode. Higher order complex modes exhibit this same property. Since complex modes

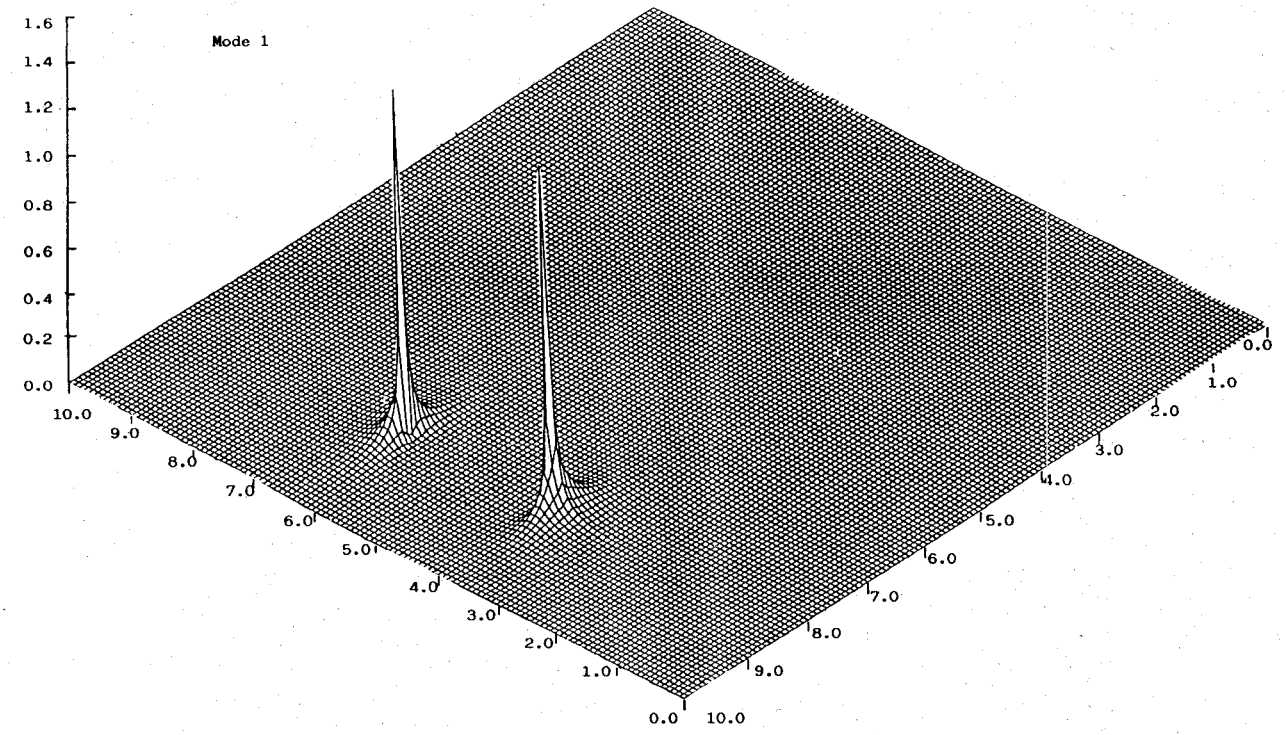

(a)

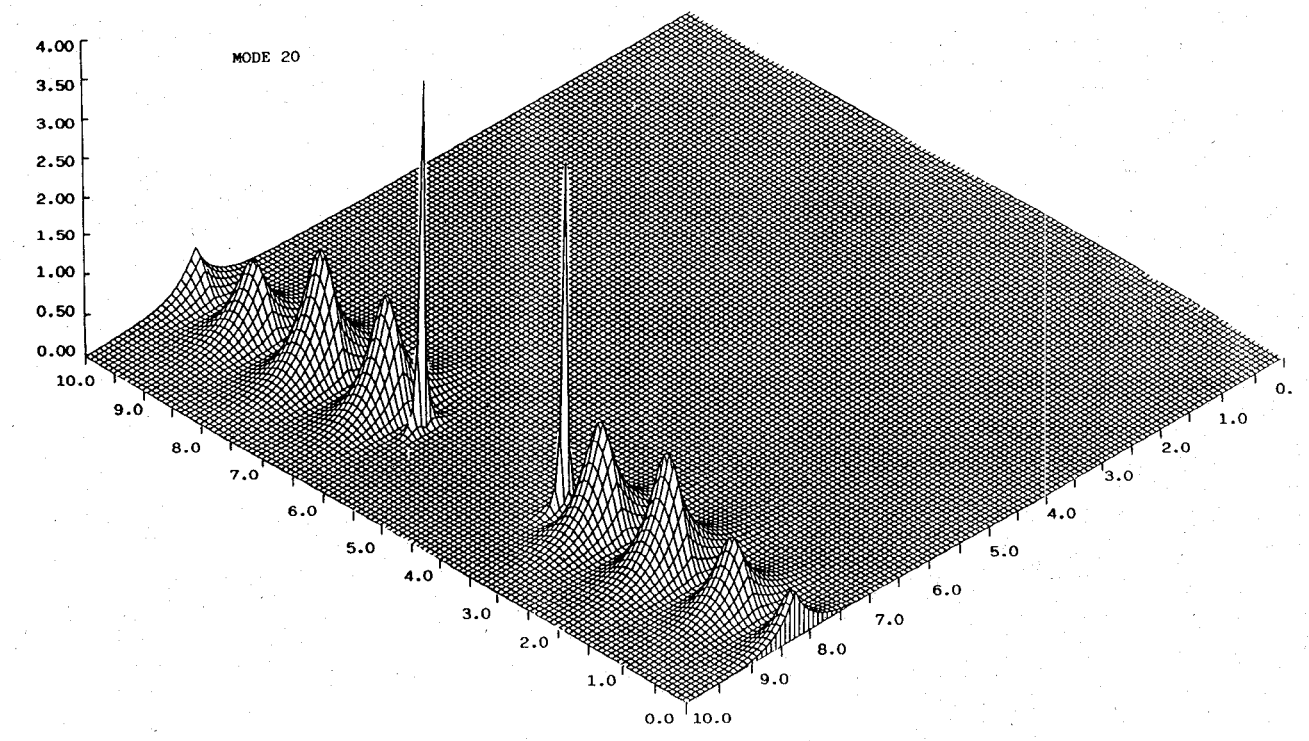

(b)

Fig. 4. (a) Transverse field intensity versus microstrip cross section. (b) Transverse field intensity versus microstrip cross section.

occur as low as the 18th, it is necessary to include them in a discontinuity calculation.

It is expected from theoretical considerations [18] that the microstrip modes will form a complete orthogonal set of functions whose domain is the guide cross section and which satisfy the boundary conditions. The following orthogonality condition applies:

$$\int \boldsymbol{E}_n(x, y) \times \boldsymbol{H}_m(x, y)\, dx\, dy = K_n \delta_{nm} \tag{12}$$

where n and m are the mode numbers of the strip, and K_n is a complex number. The above integral has been calcu-

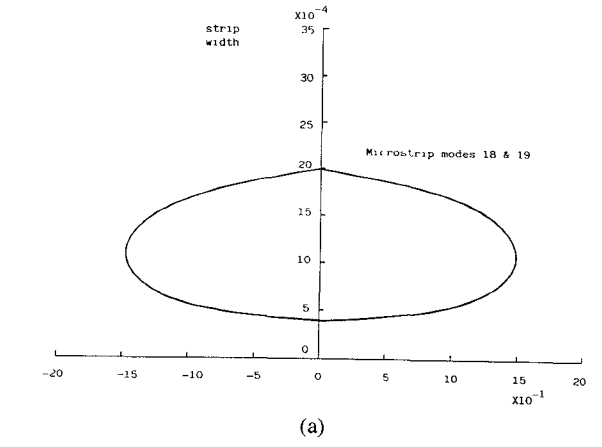

Fig. 5. (a) Effective permittivity (imag.) $(\beta/k_0)^2$. (b) Effective permittivity (real) $(\beta/k_0)^2$.

lated using the method described in Appendix III for the first 25 noncomplex modes of a microstrip. The results, which show that the calculated modes are indeed orthogonal, are shown in Table I.

This contrasts with the situation recently reported for finline [7], where a large number of basis functions are required when using the spectral domain method to calculate accurate field patterns.

Equation (12) is valid for both complex and normal modes except at the points where the modes are degenerate.

Fig. 6 shows the calculated characteristic impedance of the microstrip whose geometry is given in Fig. 2 and with a strip width of 1.27 mm. It can be seen that after an initial reduction of impedance with frequency, the impedance steadily increases with frequency. This is in agreement with other published rigorous results [16], [17] and does not agree with quasi-static formulas [1], [2] except in the low frequency limit. Fig. 7 shows the behavior of the characteristic impedance for various strip widths. For ease of comparison, the impedances have been normalized to their value in the limit of zero frequency. It can be seen that the position of the minimum is independent of the strip width.

TABLE I
MODULUS OF THE MODE COUPLING INTEGRALS FOR THE FIRST 24 MODES OF MICROSTRIP

	1	2	3	4	5	6	7	8	9	10	11	12
1	1	4e-4	3e-4	6e-4	1e-4	5e-4	2e-4	4e-4	5e-4	1e-3	2e-4	1e-4
2	2e-4	1	2e-5	4e-5	7e-6	3e-5	1e-5	3e-5	3e-5	8e-5	1e-5	1e-5
3	2e-4	2e-5	1	3e-5	6e-6	2e-5	1e-5	2e-5	3e-5	6e-5	8e-6	8e-6
4	2e-3	2e-4	1e-4	1	5e-5	2e-4	9e-5	2e-4	2e-4	5e-4	7e-5	6e-5
5	2e-4	2e-5	2e-5	4e-5	1	3e-5	1e-5	3e-5	3e-5	7e-5	9e-6	9e-6
6	1e-4	1e-5	9e-6	2e-5	3e-6	1	7e-6	1e-5	2e-5	4e-5	5e-6	5e-6
7	5e-4	5e-5	4e-5	9e-5	2e-5	7e-5	1	7e-5	8e-5	2e-4	2e-5	2e-5
8	2e-5	2e-6	2e-6	4e-6	7e-7	3e-6	1e-6	1	4e-6	8e-6	1e-6	1e-6
9	2e-3	2e-4	2e-4	4e-4	7e-5	3e-4	1e-4	3e-4	1	8e-4	1e-4	1e-4
10	5e-5	5e-6	4e-6	8e-6	1e-6	7e-6	3e-6	6e-6	7e-6	1	2e-6	2e-6
11	3e-5	3e-6	2e-6	5e-6	9e-7	4e-6	2e-6	4e-6	4e-6	1e-5	1	1e-6
12	5e-4	5e-5	4e-5	9e-5	1e-5	7e-5	3e-5	6e-5	7e-5	2e-4	2e-5	1
13	1e-4	1e-5	1e-5	2e-5	4e-6	2e-5	8e-6	2e-5	2e-5	5e-5	6e-6	6e-6
14	2e-3	3e-4	2e-4	5e-4	8e-5	3e-4	1e-4	3e-4	4e-4	9e-4	1e-4	1e-4
15	1e-4	1e-5	9e-6	2e-5	3e-6	1e-5	7e-6	1e-5	2e-5	4e-5	5e-6	5e-6
16	7e-4	7e-5	5e-5	1e-4	2e-5	9e-5	4e-5	8e-5	1e-4	2e-4	3e-5	3e-5
17	2e-4	2e-5	2e-5	4e-5	7e-6	3e-5	1e-5	3e-5	4e-5	8e-5	1e-5	1e-5
18	5e-4	5e-5	4e-5	9e-5	2e-5	7e-5	3e-5	6e-5	7e-5	2e-4	2e-5	2e-5
19	9e-4	9e-5	7e-5	2e-4	3e-5	1e-4	5e-5	1e-4	1e-4	3e-4	4e-5	4e-5
20	7e-4	6e-5	5e-5	1e-4	2e-5	9e-5	4e-5	8e-5	9e-5	2e-4	3e-5	3e-5
21	5e-4	5e-5	4e-5	9e-5	1e-5	7e-5	3e-5	6e-5	7e-5	2e-4	2e-5	2e-5
22	2e-4	2e-5	2e-5	4e-5	7e-6	3e-5	1e-5	3e-5	3e-5	8e-5	1e-5	1e-5
23	4e-3	4e-5	3e-4	8e-4	1e-4	6e-4	2e-4	5e-4	6e-4	1e-3	2e-4	2e-4
24	5e-5	5e-6	4e-6	8e-6	1e-6	7e-6	3e-6	6e-6	7e-6	2e-5	2e-6	2e-6
25	5e-4	5e-5	4e-5	8e-5	1e-5	6e-5	3e-5	6e-5	7e-5	2e-4	2e-5	2e-5

	13	14	15	16	17	18	18	20	21	22	23	24	25
1	6e-4	4e-4	2e-3	5e-5	2e-3	2e-5	1e-4	3e-4	2e-5	2e-3	4e-4	5e-5	4e-3
2	4e-5	3e-5	1e-4	3e-6	1e-4	1e-6	9e-6	2e-5	1e-6	1e-6	2e-5	3e-6	2e-4
3	3e-5	2e-5	1e-4	2e-6	9e-5	1e-6	7e-6	1e-5	1e-6	8e-5	2e-5	3e-6	2e-4
4	3e-4	2e-4	8e-4	2e-5	7e-4	1e-5	6e-5	1e-4	8e-6	7e-4	2e-4	2e-5	2e-3
5	4e-5	3e-5	1e-4	3e-6	1e-4	1e-6	8e-6	2e-5	1e-6	1e-6	2e-5	3e-6	2e-4
6	2e-5	1e-5	6e-5	2e-6	6e-5	7e-7	4e-6	9e-6	6e-7	5e-5	1e-5	2e-6	1e-4
7	1e-4	7e-5	3e-4	7e-6	2e-4	3e-6	2e-5	4e-5	3e-6	2e-4	6e-5	8e-6	6e-4
8	4e-6	3e-6	1e-5	3e-7	1e-5	1e-7	9e-7	2e-6	1e-7	1e-5	2e-6	3e-7	3e-5
9	4e-4	3e-4	1e-3	3e-5	1e-3	1e-5	9e-5	2e-4	1e-5	1e-3	2e-4	3e-5	3e-3
10	9e-6	6e-6	3e-5	7e-7	2e-5	3e-7	2e-6	4e-6	3e-7	2e-5	5e-6	7e-7	5e-5
11	6e-6	4e-6	2e-5	4e-7	1e-5	2e-7	1e-6	2e-6	2e-7	1e-5	3e-6	4e-7	3e-5
12	9e-5	6e-5	3e-4	7e-6	2e-4	8e-4	3e-6	2e-5	4e-5	3e-6	2e-4	5e-5	5e-4
13	1	2e-5	7e-5	2e-6	6e-5	8e-7	5e-6	1e-5	7e-7	6e-5	1e-5	2e-6	1e-4
14	5e-4	1	1e-3	4e-5	1e-3	2e-5	1e-6	2e-4	1e-5	1e-3	3e-4	4e-5	3e-3
15	2e-5	1e-5	1	2e-6	6e-5	7e-7	4e-6	9e-6	6e-7	5e-5	1e-5	2e-6	1e-4
16	1e-4	8e-5	3e-4	1	3e-4	4e-6	2e-5	5e-5	3e-6	3e-4	7e-5	6e-6	7e-4
17	4e-5	3e-5	1e-4	3e-6	1	1e-6	9e-6	2e-5	1e-6	1e-4	2e-5	3e-6	3e-4
18	9e-5	6e-5	3e-4	7e-6	2e-4	1	2e-5	4e-5	3e-6	2e-4	5e-5	7e-6	5e-4
19	2e-4	1e-4	5e-4	1e-5	4e-4	6e-6	1	7e-5	5e-6	4e-4	9e-5	1e-5	1e-3
20	1e-4	8e-5	3e-4	8e-6	3e-4	4e-6	2e-5	1	3e-6	3e-4	7e-5	9e-6	7e-4
21	9e-5	6e-5	3e-4	6e-6	2e-4	3e-6	2e-5	4e-5	1	2e-4	5e-5	7e-6	5e-4
22	4e-5	3e-5	1e-4	3e-6	1e-4	1e-6	8e-6	2e-5	1e-6	1	2e-5	3e-6	2e-4
23	8e-4	5e-4	2e-3	6e-5	2e-3	3e-5	2e-4	3e-4	2e-5	2e-3	1	6e-5	4e-3
24	8e-6	6e-6	2e-5	6e-7	2e-5	3e-7	2e-6	4e-6	2e-7	2e-5	5e-6	1	5e-5
25	8e-5	6e-5	2e-4	6e-6	2e-4	3e-6	2e-5	4e-5	2e-6	2e-4	5e-5	7e-6	1

$a = 34$ mm; $d = 3.175$ mm; $b = 34$ mm; $\epsilon_r = 2.33$; $w = 4.2$ mm. Frequency = 3 GHz.

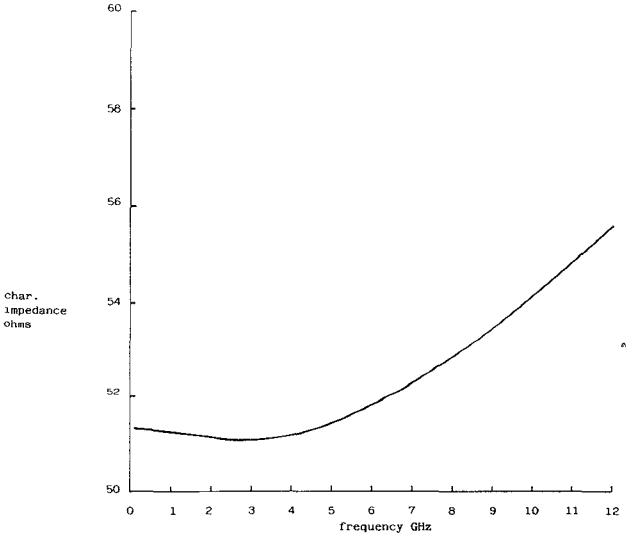

Fig. 6. Characteristic impedance of microstrip. $a = 12.7$ mm; $d = 1.27$ mm; $h = 10.43$ mm; $w = 1.27$ mm; eps = 8.875.

V. CONCLUSIONS

In this paper we have presented an efficient method of calculating the propagation coefficients and field patterns of the higher order modes of microstrip. This includes the

"complex modes" as well as the usual evanescent modes. The computation required is small enough to make it entirely practicable to perform the calculations on a "home computer." In addition the method has been used to calculate the characteristic impedance of microstrip. The results of these calculations are in a form suitable for use in the characterization of strongly coupled microstrip discontinuities.

Appendix I

The Fourier transforms of the quantities in (5) are given by

$$\tilde{J}_z(n) = \int_{-a/2}^{a/2} J_z(x) \sin \frac{n\pi(x-a/2)}{a}\, dx$$

$$\tilde{J}_x(n) = \int_{-a/2}^{a/2} J_x(x) \cos \frac{n\pi(x-a/2)}{a}\, dx$$

$$\tilde{g}_{zz}(n,\beta) = \int\int\int\int g_{zz}(r,r') \sin \frac{n\pi(x-a/2)}{a} \cdot \sin \frac{n\pi(x'-a/2)}{a} \exp(-j\beta z) \cdot \exp(-j\beta z')\, dx\, dx'\, dz\, dz'$$

$$\tilde{g}_{zx}(n,\beta) = \int\int\int\int g_{zx}(r,r') \sin \frac{n\pi(x-a/2)}{a} \cdot \cos \frac{n\pi(x'-a/2)}{a} \exp(-j\beta z) \cdot \exp(-j\beta z')\, dx\, dx'\, dz\, dz'$$

$$\tilde{g}_{xz}(n,\beta) = \int\int\int\int g_{xz}(r,r') \cos \frac{n\pi(x-a/2)}{a} \cdot \sin \frac{n\pi(x'-a/2)}{a} \exp(-j\beta z) \cdot \exp(-j\beta z')\, dx\, dx'\, dz\, dz'$$

$$\tilde{g}_{xx}(n,\beta) = \int\int\int\int g_{xx}(r,r') \cos \frac{n\pi(x-a/2)}{a} \cdot \cos \frac{n\pi(x'-a/2)}{a} \exp(-j\beta z) \cdot \exp(-j\beta z')\, dx\, dx'\, dz\, dz'.$$

We are assuming current on the strip with a z dependence of the form $\exp(-j\beta z)$.

Appendix II
Derivation of the Microstrip Green's Dyadic Impedance

We expand the fields in a shielded planar transmission line in terms of y-directed Hertzian potentials as follows:

$$E = -j\omega\mu\nabla \times \Pi_h + k^2 \Pi_e + \nabla\nabla\cdot\Pi_e \tag{A1}$$

$$H = k^2 \Pi_h + \nabla\nabla\cdot\Pi_h + j\omega\epsilon\nabla \times \Pi_e \tag{A2}$$

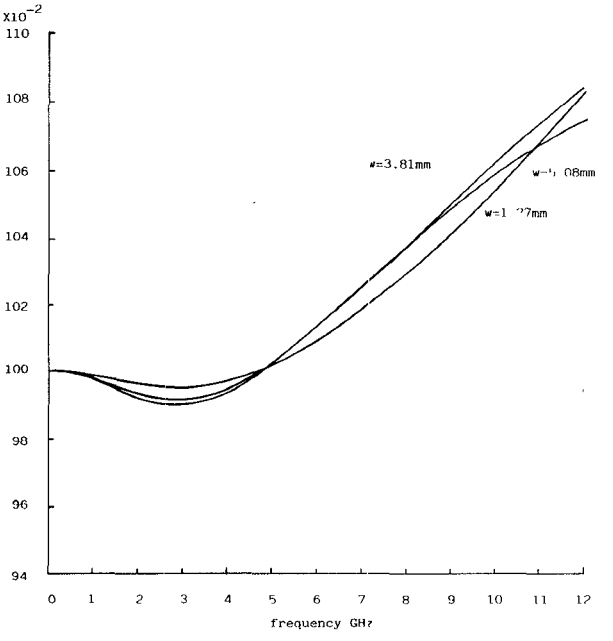

Fig. 7. Normalized characteristic impedance of microstrip. $a = 12.7$ mm; $d = 1.27$ mm; $h = 10.43$ mm; eps = 8.875.

where

$$\Pi_h = \psi_h(x,y) e^{-j\beta z}$$

$$\Pi_e = \psi_e(x,y) e^{-j\beta z}$$

$$\psi_h = \sum_{n=0}^{n=\infty} C_n \frac{\sin k_n(h+y)}{\sin k_h h} \cos\alpha_n(x+a/2), \qquad y>0 \tag{A3}$$

$$\psi_h = \sum_{n=0}^{n=\infty} D_n \frac{\sin k_n'(h'-y)}{\sin k_n' h'} \cos\alpha_n(x+a/2), \qquad y<0 \tag{A4}$$

$$\psi_e = \sum_{n=0}^{n=\infty} A_n \frac{\cos k_n(h+y)}{\cos k_n h} \sin\alpha_n(x+a/2), \qquad y>0 \tag{A5}$$

$$\psi_e = \sum_{n=0}^{n=\infty} B_n \frac{\cos k_n'(h'-y)}{\cos k_n' h'} \sin\alpha_n(x+a/2), \qquad y<0$$

$$\alpha_n = n\pi/a \tag{A6}$$

and k_n, k_n' are constrained by the relationship

$$k_n^2 = \epsilon_r k_0^2 - \beta^2 - \alpha_n^2$$

$$k_n'^2 = k_0^2 - \beta^2 - \alpha_n^2.$$

We can write the fields in the substrate as follows:

$$E_x(x) = \sum(-A_n k_n \alpha_n \tan k_n h + C_n \omega\mu_0\beta)\cos\alpha_n(x+a/2)$$

$$E_y(x) = \sum A_n(\epsilon_r k_0^2 - k_n^2)\sin\alpha_n(x+a/2)$$

$$E_z(x) = \sum(A_n k_n j\beta \tan k_n h + C_n j\omega\mu_0\alpha_n)\sin\alpha_n(x+a/2)$$

$$H_x(x) = \sum(-A_n\omega\epsilon_0\epsilon_r\beta - C_n k_n \alpha_n \cot k_n h) \cdot \sin\alpha_n(x+a/2)$$

$$H_y(x) = \sum C_n(\epsilon_r k_0^2 - k_n^2)\cos\alpha_n(x+a/2)$$

$$H_z(x) = \sum(A_n j\omega\epsilon_0\alpha_n - C_n j\beta k_n \cot k_n h)\alpha_n(x+a/2). \tag{A7}$$

Similarly in air:

$$E_x(x) = \sum \left(B_n k_n' \alpha_n \tan k_n' h' + D_n \omega \mu_0 \beta\right) \cos \alpha_n (x + a/2)$$

$$E_y(x) = \sum B_n \left(k_0^2 - k_n'^2\right) \sin \alpha_n (x + a/2)$$

$$E_z(x) = \sum \left(-B_n k_n' j\beta \tan k_n' h' + D_n j\omega \mu_0 \alpha_n\right) \cdot \sin \alpha_n (x + a/2)$$

$$H_x(x) = \sum \left(-B_n \omega \epsilon_0 \beta + D_n k_n' \alpha_n \cot k_n' h'\right) \sin \alpha_n (x + a/2)$$

$$H_y(x) = \sum D_n \left(k_0^2 - K_n'^2\right) \cos \alpha_n (x + a/2)$$

$$H_z(x) = \sum \left(B_n j\omega \epsilon_0 \alpha_n + D_n j\beta k_n' \cot k_n' h'\right) \cdot \cos \alpha_n (x + a/2). \tag{A8}$$

Applying the boundary conditions at the air–dielectric interface, we can obtain the following solutions for A, B, C, and D:

$$C_n = D_n \tag{A9}$$

$$A_n = -B_n \frac{k_n' \tan k_n' h'}{k_n \tan k_n h} \tag{A10}$$

$$D_n = \frac{-\alpha_n \tilde{J}_z + j\beta \tilde{J}_x}{\left(\alpha_n^2 + \beta^2\right)(Y)} \tag{A11}$$

$$B_n = \frac{\left(\beta \tilde{J}_z + j\alpha_n \tilde{J}_x\right) k_n \tan k_n h}{\left(\alpha_n^2 + \beta^2\right)(X) \omega \epsilon_0} \tag{A12}$$

where

$$X = \epsilon_r k_n' \tan k_n' h' + k_n \tan k_n h \tag{A13}$$

$$Y = k_n \cot k_n h + k_n' \cot k_n' h' \tag{A14}$$

$$\tilde{J}_z(n) = \int J_z(x) \sin \alpha_n (x + a/2)\, dx \tag{A15}$$

$$\tilde{J}_x(n) = \int J_x(x) \cos \alpha_n (x + a/2)\, dx. \tag{A16}$$

The integrals are taken over the strips since no current flows where there is no strip.

We now substitute into the equations for the x and z components of the fields and get an expanded version of (1):

$$E_z(x) = \sum_n \left(G_{zz} \tilde{J}_z + \frac{G_{zx}}{\alpha_n} \tilde{J}_x'\right) \sin \alpha_n (x + a/2) \tag{A17}$$

$$E_x(x) = \sum_n \left(G_{xz} \tilde{J}_z + \frac{G_{xx}}{\alpha_n} \tilde{J}_x'\right) \cos \alpha_n (x + a/2) \tag{A18}$$

where

$$G_{zz} = \frac{-j\left(\left(\epsilon_r k_0^2 - \beta^2\right) k_n' \tan k_n' h' + \left(k_0^2 - \beta^2\right) k_n \tan k_n h\right)}{\det}$$

$$G_{zx} = G_{xz} = -\frac{B\alpha_n \left(k_n' \tan k_n' h' + k_n \tan k_n h\right)}{\det}$$

$$G_{xx} = \frac{j\left(\left(\epsilon_r k_0^2 - \alpha_n^2\right) k_n' \tan k_n' h' + \left(k_0^2 - \alpha_n^2\right) k_n \tan k_n h\right)}{\det}$$

$$\det = \omega \epsilon_0 (X)(Y).$$

As n approaches infinity k_n and k_n' approach $j\alpha_n$, and $\tan j\alpha_n h$ approaches 1; therefore the asymptotic limit of the Green's function is

$$H_{zz} = G_{zz} \to j\beta^2/(1 + \epsilon_r)$$

$$H_{zx} = G_{zx}/\alpha_n = G_{xz}/\alpha_n \to -\beta/2(1 + \epsilon_r)$$

$$H_{xx} = G_{xx}/\alpha_n^2 \to -j/2(1 + \epsilon_r).$$

The dyadic $\underline{\underline{H}}(\beta)$ is defined as

$$\begin{Bmatrix} H_{xx} & H_{xz} \\ H_{zx} & H_{zz} \end{Bmatrix}.$$

Appendix III
Computation of Inner Products

In order to show that the calculated field patterns are orthogonal, as required by theory, we are required to calculate the inner products of the microstrip modal fields. To keep the discussion general, we will not require the field patterns to be modes of the same microstrip. The inner products are calculated as follows:

$$P = \int\int (\boldsymbol{E} \times \boldsymbol{H}) \cdot \tilde{z}\, dx\, dy$$

$$= \int\int \left(E_x H_y - E_y H_x\right) dx\, dy. \tag{A19}$$

From the results of the previous analysis we have expressions for the E and H fields in the following form:

$$E_x = \sum_n \tilde{E}_{xn}^+(n) \cos \alpha_n (x + a/2) \frac{\sin k_n'(h - y)}{\sin k_n' h}, \qquad y > 0$$

$$E_x = \sum_n \tilde{E}_{xn}^-(n) \cos \alpha_n (x + a/2) \frac{\sin k_n (d + y)}{\sin k_n d}, \qquad y < 0 \tag{A20}$$

and similarly for the other components.

It is noted that H_x and E_y are discontinuous at the interface between air and substrate. Thus we must use the coefficients appropriate to the region. The superscript + on the coefficients indicates that they apply to the air region ($y > 0$) while the superscript − indicates that they apply to the substrate region ($y < 0$).

If we split the inner product into two parts thus:

$$P = P_x - P_y \tag{A21}$$

where

$$P_x = \int\int E_x H_y\, dx\, dy$$

$$P_y = \int\int E_y H_x\, dx\, dy$$

we get for each part an expression of the following form:

$$P_i = \sum_n \sum_m A_n^+ B_m^+ \int_0^a T(\alpha_n x) T(\alpha_m x)\, dx \cdot \int_0^h \frac{U(k_n'(h-y)) U(k_m'(h-y))\, dy}{U(k_n' h) U(k_m' h)} + \sum_n \sum_m A_n^- B_m^- \int_0^a T(\alpha_n x) T(\alpha_m x)\, dx \cdot \int_{-d}^0 \frac{U(k_n(d+y) U(k_m(d+y))\, dy}{U(k_n d) U(k_m h)} \quad \text{(A22)}$$

where T and U are either sin or cos depending on which field components are being used, and A and B are the appropriate field coefficients.

This becomes

$$\sum_n \tau_n \left\{ \frac{A_n^- B_n^- I_1}{U(k_{n1} d) U(k_{n2} d)} + \frac{A_n^+ B_n^+ I_2}{U(k_{n1}' h) U(k_{n2}' h)} \right\} \quad \text{(A23)}$$

where

$$I_1 = \int_{-d}^0 [\cos(k_{n1} + k_{n2})(d+y) -/+ \cos(k_{n1} + k_{n2})(d+y)]\, dy$$

$$I_2 = \int_0^h [\cos(k_{n1}' - k_{n2}')(h-y) -/+ \cos(k_{n1}' + k_{n2}')(h-y)]\, dy$$

where

$$\tau_n = a \quad \text{if } n = 0$$
$$= a/2 \quad \text{if } n > 0.$$

The first signs are taken if U is sin, the second if U is cos. The quantities k_{n1}, k_{n1}' are the propagation constants for the y direction is defined in Appendix II for the first field pattern; k_{n2}, k_{n2}' are the corresponding propagation constants for the second field pattern. The result of doing the integrals is

$$I_1 = \frac{\sin(k_{n2} - k_{n2}) d}{k_{n2} - k_{n2}} -/+ \frac{\sin(k_{n1} + k_{n2}) d}{k_{n1} + k_{n2}}$$

$$I_2 = \frac{\sin(k_{n1}' - k_{n2}') h}{k_{n1}' - k_{n2}'} -/+ \frac{\sin(k_{n1}' + k_{n2}') h}{k_{n1}' + k_{n2}'}.$$

By expanding the sin terms and substituting into (A23), we find that the inner product is

if U is sin:

$$\sum A_n^- B_n^- \tau_n \frac{k_{n2} \cot k_{n2} d - k_{n1} \cot k_{n1} d}{k_{n1}^2 - k_{n2}^2} + \sum A_n^+ B_n^+ \tau_n \frac{k_{n2}' \cot k_{n2}' h - k_{n1}' \cot k_{n1}' h}{k_{n1}'^2 - k_{n2}'^2}$$

if U is cos:

$$\sum A_n^- B_n^- \tau_n \frac{k_{nz} \tan k_{n2} d - k_{n1} \tan k_{n1} d}{k_{n1}^2 - k_{n2}^2} + \sum A_n^+ B_n^+ \tau_n \frac{k_{n2}' \tan k_{n2}' h - k_{n1}' \tan k_{n1}' h}{k_{n1}'^2 - k_{n2}'^2}.$$

We define the functions $P(Z1, Z2, X)$ and $Q(Z1, Z2, X)$ as follows:

$$P(Z1, Z2, X) = \frac{Z2 \cot Z2.X - Z1 \cot Z1.X}{Z1^2 - Z2^2}, \quad Z1^2 \neq Z2^2$$
$$= \frac{1}{2} \left\{ \frac{X}{\sin^2 Z1.X} - \frac{1}{Z1 \tan Z1.X} \right\}, \quad Z1^2 = Z2^2$$

$$Q(Z1, Z2, X) = \frac{Z1 \tan Z2.X - Z2 \tan Z1.X}{Z1^2 - Z2^2}, \quad Z1^2 \neq Z2^2$$
$$= \frac{1}{2} \left\{ \frac{X}{\cos^2 Z1.X} + \frac{1}{Z1 \cot Z1.X} \right\}, \quad Z1^2 = Z2^2.$$

Then the Poynting vector P is equal to

$$a\tau_n \sum_n E_{xn}^+ H_{yn}^+ P(k_{n1}', k_{n2}', h) + a\tau_n \sum_n E_{xn}^- H_{yn}^- P(k_{n1}, k_{n2}, d) - a\tau_n \sum_n E_{yn}^+ H_{xn}^+ Q(k_{n1}', k_{n2}', h) - a\tau_n \sum_n E_{yn}^- H_{xn}^- Q(k_{n1}, k_{n2}, d).$$

References

[1] K. C. Gupta *et al.*, *Computer Aided Design of Microwave Circuits*. Dedham, MA: Artech, 1981.

[2] R. Hoffman, *Integrierte Mikrowellenschaltungen*. Berlin: Springer-Verlag, 1983.

[3] R. Mehran, *Grundelemente des rechnergestützten Entwurfs von Mikrostreifenleitungs-Schaltungen*. Aachen: Verlag H. Wolff, 1983, ch. 5.

[4] N. Koster and R. H. Jansen "The microstrip discontinuity—A revised description," *IEEE Trans. Microwave Theory Tech.*, vol. MTT-34, pp. 213–223, Feb. 1986.

[5] L. P. Schmidt, "Rigorous computation of the frequency dependent properties of filters and coupled resonators composed from transverse microstrip discontinuities," in *Proc. 10th European Microwave Conf.* (Warsaw), 1980, pp. 436–440.

[6] C. J. Railton, T. Rozzi, and J. Kot, "The efficient calculation of high order microstrip modes for use in discontinuity problems," in *Proc. 16th European Microwave Conf.*, 1986, pp. 529–534.

[7] A. S. Omar and K. F. Schünemann, "Formulation of the singular equation technique for planar transmission lines," *IEEE Trans. Microwave Theory Tech.*, vol. MTT-33, p. 1313, Dec. 1985.

[8] T. Itoh and R. Mittra, "Technique for computing dispersion characteristics of shielded microstrip lines," *IEEE Trans. Microwave Theory Tech.*, vol. MTT-22, pp. 896–898, Oct. 1974.

[9] T. Itoh, "Spectral domain immittance approach for dispersion characteristics of generalized printed transmission lines," *IEEE Trans. Microwave Theory Tech.*, vol. MTT-28, pp. 733–736, July 1980.

[10] C. A. Olley and T. Rozzi, "Systematic characterisation of the spectrum of unilateral finline," *IEEE Trans. Microwave Theory Tech.*, vol. MTT-34, pp. 1147–1156, Nov. 1986.

[11] E. J. Denlinger, "A frequency dependent solution for microstrip transmission lines," *IEEE Trans. Microwave Theory Tech.*, vol. MTT-19, pp. 30–39, Jan. 1971.

[12] R. H. Jansen and M. Kirschning, "Arguments and an accurate model for the power–current formulation on microstrip characteristic impedance," *Arch. Elek. Übertragung*, vol. 37, pp. 108–112, 1983.

[13] W. J. Getsinger, "Measurement and modelling of the apparent characteristic impedance of microstrip," *IEEE Trans. Microwave Theory Tech.*, vol. MTT-31, pp. 624–632, Aug. 1983.
[14] E. F. Kuester *et al.*, "Frequency dependent definitions of microstrip characteristic impedance," in *Dig. Int. URSI Symp. Electromagnetic Waves* (Munich), 1980, pp. 355B1–3.
[15] F. Arndt and G. U. Paul, "The reflection definition of the characteristic impedance of microstrip," *IEEE Trans. Microwave Theory Tech.*, vol. MTT-27, pp. 724–731, Aug. 1979.
[16] H. Y. Yee and K. Wu, "Printed circuit transmission-line characteristic impedance by transverse modal analysis," *IEEE Trans. Microwave Theory Tech.*, vol. MTT-33, pp. 1157–1163, Nov. 1985.
[17] M. Hashimoto, "A rigorous solution for dispersive microstrip," *IEEE Trans. Microwave Theory Tech.*, vol. MTT-33, pp. 1131–1137, Nov. 1985.
[18] R. E. Collin, *Field Theory of Guided Waves*. New York McGraw Hill, 1960.
[19] A. S. Omar and K. Schünemann, "On the numerical determination of guiding resonance and radiation modes in planar structures," in *Symp. Dig. IEEE AP-S Symp.* (Philadelphia), 1986, pp. 481–484.

C. J. Railton was born in Walsall, Staffordshire, England, in 1952. He received the B.Sc. degree (with honors) in physics with electronics from the University of London in 1974.

During the years 1974–1984 he worked in the scientific civil serve on a number of research and development projects in the areas of communications and signal processing. In 1987 he completed the Ph.D. degree at the University of Bath on boxed microstrip circuits. He is currently a lecturer in the Department of Electrical Engineering at Bristol University.

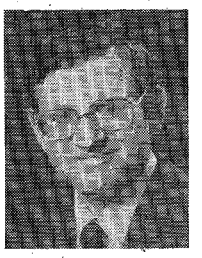

T. Rozzi (M'66–SM'74) obtained the degree of "Dottore" in physics from the University of Pisa in 1965 and the Ph.D. degree in electronic engineering at Leeds University in 1968. In June 1987 he received the degree of D.Sc. from the University of Bath.

From 1968 to 1978 he was a Research Scientist at the Philips Research Laboratories, Eindhoven, the Netherlands, having spent one year in 1975 at the Antenna Laboratory, University of Illinois, Urbana.

In 1975 he was awarded the Microwave Prize of the Microwave Theory and Technique Group of the Institute of Electrical and Electronics Engineers. In 1978 he was appointed to the Chair of Electrical Engineering at the University of Liverpool and subsequently appointed to the Chair of Electronics and Headship of the Electronics Group at the University of Bath in 1981. From 1983 to 1986 he held the additional responsibility of Head of the School of Electrical Engineering at Bath. Since 1986 Dr. Rozzi has also held the "ordinary chair" of Antennas at the Faculty of Engineering, University of Ancona, Italy.